From polymer–metal complex framework to 3D architectures: growth, characterization and formation mechanism of micrometer-sized α-NiS

Fen Xu, Yi Xie,* Xu Zhang, Changzheng Wu, Wang Xi, Jie Hong and Xiaobo Tian

Structure Research Lab and Department of Chemistry, University of Science & Technology of China, Hefei, Anhui 230026, P. R. China. E-mail: yxielab@ustc.edu.cn; Fax: 86-551-3603987; Tel: 86-551-3603987

Received (in Montpellier, France) 28th March 2003, Accepted 26th May 2003
First published as an Advance Article on the web 15th August 2003

A complex-ion reaction route under solvothermal conditions was investigated for the preparation of micrometer-sized NiAs-type α-NiS with complex architectures, on the basis of the strategy that the framework structure of PEG-$NiCl_2$ complex could provide orientation for the growth of 3D NiAs-type α-NiS crystals. The as-prepared NiS powders with flower-like architectures were characterized by X-ray diffraction pattern (XRD), field emission scanning electron microscopy (FE-SEM), ultraviolet, visible light (UV-Vis) and photoluminescence (PL) spectra. Fourier transform infrared absorption (FT-IR) spectra as functions of temperature were recorded to investigate the coordinative chemical effect in the PEG–$NiCl_2$ complex. When PEG-6000 was substituted with poly(vinyl alcohol) (PVA) or poly(vinyl pyrrolidone) (PVP), two other complex architectures (*i.e.* tennis-ball shaped or urchin-like) were produced. On the basis of a series of supplementary experiments and the result of FT-IR spectra, it was found that both the framework structure of the polymer–metal complex and the functional groups on the polymers had a considerable effect on the final architectures of α-NiS crystals.

Introduction

Nanomaterials and the patterned aggregation of small particles are promising candidates in several fields of application and thus the building and patterning of inorganic nanoparticles into 2D and 3D organized structures by manipulation of individual units is a potential route to utilizing their chemical, optical, catalytic, magnetic and electronic properties.[1,2] Recently, several methods have been attempted for the synthesis of inorganic materials with complex patterns and much use has been made of polymers, including poly(ethylene glycol) (PEG) and its block copolymers, as the crystal morphology-modifiers.[3–7] For example, wire- or rod-like Cu_2O has been fabricated with PEG-400,[3] rod-like Ag or cubic Cu_2O has been prepared in the presence of PEG-20000 and oriented mesoporous WO_3 films have been synthesized involving the use of PEG-300.[4] We also previously used the PEG-2000 polymer to synthesize Ag nanowire at 90 °C and granular, needle-, rod-, or whisker-shaped γ-Fe_2O_3 nanocrystals *via* γ-irradiation. In addition, $BaSO_4$, $CdWO_4$, $BaCrO_4$ and $CaC_2O_4{\cdot}2H_2O$ with intricate or elegant morphologies are successfully displayed in the presence of PEG-block copolymers.[6,7] With careful choice of PEG polymer, we find that PEG distinguishes itself as a morphology modifier having at least the following three characteristics: First, it has a wide molecular weight distribution, generally speaking in the range of 200∼20 000. The more or less extended order of the polymer chain or framework could provide a new sort of organization to metal atoms along the polymer backbone, affording diverse ways of assemblage for the final products. Secondly, it can combine with other polymers to form double-hydrophilic block copolymers, providing more complex structures and further candidates as morphology-directors. Thirdly, due to the lone pair electrons on the oxygen atoms, PEG can act as a donor to the metal ions with vacant d-orbit and combine with metal ions to form the complexes with various conformations, and thus control the morphology of the final products. All these studies give us the inspiration that it is possible to build new 3D architectures when using PEG with appropriate molecular weights.

Metal chalcogenides have received much more attention in the field of materials science[8] because of their unusual electronic properties and interesting chemical behavior. Of the binary sulfides, nickel monosulfide (NiS) has been the subject of considerable interest due to its unique electromagnetic property of a first-order phase transition from a low-temperature antiferromagnetic semiconductor to a high-temperature paramagnetic metal, and its use as a hydro-desulfurization catalyst, and in cathodic materials and solar storage.[9–11] As a catalyst, NiS with 2D or 3D organized structures maybe provides the directional catalyst ability. However, as to NiS, how atoms or building blocks can be rationally assembled into 3D microstructures is a challenging issue presently faced by chemists. Here, we chose a facile complex-ion reaction route to synthesize 3D NiAs-type NiS with complex architectures, in which the framework structure of the PEG–$NiCl_2$ complex provides a way to grow 3D micrometer-sized NiS crystals. Furthermore, the possible mechanism of formation of the 3D complexes architectures was studied on the basis of a series of supplementary experiments and the results of FT-IR spectra of the PEG–$NiCl_2$ complex.

Experimental

Synthesis of flower-like α-NiS architectures

In a typical procedure for the preparation of the flower-like NiS, two steps were needed: **I**. The preparation of the

$PEG–NiCl_2$ complex. 0.39 g (3 mmol) nickel chloride ($NiCl_2$), 1.8 g (0.3 mmol) polyethylene glycol (PEG, molecular weight = 6000), 30 mL ethanol (C_2H_5OH) and 10 mL butylacetate ($CH_3COOC_4H_9$) were mixed and stirred for 3 h, the color of the mixture turning to yellow-green. Here, the temperature should be kept at 60–70 °C when stirring, since if the temperature falls below this the $PEG–NiCl_2$ complex precipitates from the mixed solution. **II**. The preparation of the flower-like NiS powders. After 0.226 g (3 mmol) thioacetamide (CH_3CSNH_2) and 5 mL distilled water were added to the above system and stirred for further 1 h at 60–70 °C, a clear absinthe-green solution resulted. This solution was transferred to a Teflon-lined stainless steel autoclave of 50 mL capacity (filled to 95% of its total volume). The autoclave was maintained at 150 °C for 9 h and then allowed to cool naturally to room temperature . The precipitates were filtered and washed with distilled water and absolute ethanol successively, and finally the brown-black precipitates were dried under vacuum at 60 °C for 3 h.

Characterization techniques

The composition of the as-prepared product was determined by X-ray powder diffraction (XRD), using a Philip X′ Pert PRO SUPER rA rotation anode with Ni-filtered Cu Kα radiation (λ = 1.541874 Å) at 25 °C. X-ray photoelectron spectroscopy (XPS) was performed on ESCALAB MKII with MgK_α (hv = 1253.6 eV) as the exciting source. The binding energies obtained in the XPS analysis were corrected for specimen charging by referencing the C_{1s} to 284.5 eV. Field emission scanning electron microscopy (FE-SEM) was taken on a JEOL JSM-6700F SEM. The UV-Vis absorption was recorded on a UV-Vis spectrophotometer Specord 200 (Analytic Jena AG) absorption diode array spectrometer using 1 cm quartz curettes. Fluorescence was determined by a Hitachi 850-luminescence spectrophotometer with a Xe lamp at 25 °C (λ_{ex} = 274.2 nm). FT-IR spectra were recorded on a Nicolet Model 759 Fourier Transmission Infrared spectrometer, at wavenumbers 500–4000 cm^{-1}.

Results and discussion

Phase and morphology of the products

The XRD pattern in Fig. 1a demonstrates that well-crystallized NiS powders can be easily synthesized at 150 °C, which can be indexed as hexagonal NiAs-type α-NiS phase with unit cell parameters a = 9.637 Å, c = 3.123 Å (JCPDS Card 12–41). It is worth noting that the ratio between the intensities of (101) and (300) diffraction peak (1.00 *versus* 0.50) is much higher than the conventional value (0.40 *versus* 1.00), indicating that our samples tend to be preferentially oriented. The composition and the purity of the products are examined by X-ray photoelectron spectroscopy (XPS). The binding energy values of ~856.2 eV for $Ni_{2p3/2}$ and that of ~161.9 eV for S_{2p} are authenticated by the XPS spectra. The ratio of integral area for $Ni_{2p3/2}$ to S_{2p} is about 0.96 : 1. These results are in good agreement with the reported data of NiS.[12]

The product morphologies are determined by field emission scanning electron microscopy (FE-SEM). Fig. 1b–c depicts the FE-SEM images showing micrometer-sized NiS with flower-like architectures. As shown in Fig. 1b, the flower-like NiS crystals are uniform in size and most are in the range ~16–18 μm. Fig. 1c (the inset) presents a high-magnification FE-SEM image of a single flower-like morphology, revealing that the elegant architecture consists of crispate sheets. FE-SEM images show these crispate sheets grow larger and larger from the inner to the outer, which suggest that the crystals grow along a certain direction after a nucleation process. It can be observed that the flower-like morphology shows a faceted surface, indicating that it is composed of larger crystals. This is consistent with the XRD pattern that exhibited relative sharp NiS diffraction peaks.

Optical properties

UV-Vis absorption and fluorescence properties of the flower-like NiS powders are measured. Fig. 2a shows the absorption spectrum of the sample dispersed in ethanol by sonication. The peak in Fig. 2a is centered at ~497 nm (~2.50 eV), which is blue-shifted ~0.40 eV over bulk NiS (~2.10 eV).[13] Higher energy transitions (~2.50 eV) are attributed to the first excitonic peak of NiS in the absorption spectrum. And the remarkable blue shift for the flower-like NiS is probably attributable to the small dimension of the NiS "bricks" of the sheet, which is similar to the reported result.[1a,10b] Fig. 2b shows the fluorescence spectrum of the sample (λ_{ex} = 274.2 nm), which consists of a broad emission with a maximum at 406 nm (~3.05 eV).

Formation mechanism of α-NiS phase

The formation of NiS is based on the reactions among $NiCl_2$, PEG, CH_3CSNH_2 and H_2O, which can be described as follows:

$$PEG + NiCl_2 \xrightarrow{333\text{-}343\ K} PEG - NiCl_2\ (complex) \quad (1)$$

$$CH_3CSNH_2 + 2H_2O \xrightarrow{heating} H_2S + CH_3COOC_2H_5 \quad (2)$$

$$PEG - NiCl_2(complex) + H_2S \rightarrow NiS + 2HCl + PEG \quad (3)$$

The reaction of $PEG–NiCl_2$ complex with H_2S under heating can give rise to brown-black NiS precipitates.

Fourier transform infrared absorption (FT-IR) spectra

In our experiments, it is of paramount importance for the $PEG–NiCl_2$ complex to discuss the coordinative chemical

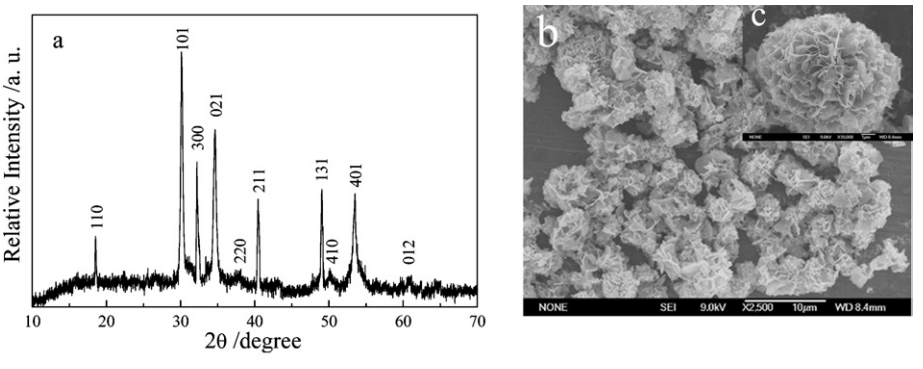

Fig. 1 (a) XRD pattern of the synthetic α-NiS powders obtained in the presence of PEG-6000 polymer; (b) FE-SEM image of flower-like NiS powders with rather uniform size; (c) the inset is a high-magnification FE-SEM image exhibiting a flower-like architecture.

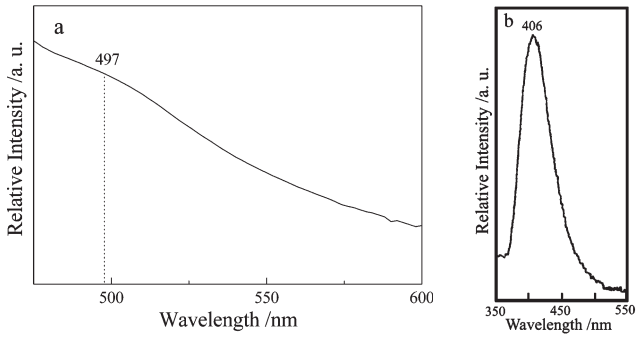

Fig. 2 (a) UV-Vis absorption spectrum and (b) fluorescence spectrum (λ_{ex} = 274.2 nm) of the flower-like NiS crystals.

effect between PEG and $NiCl_2$. To investigate the coordinative effect between PEG and Ni^{2+} ions, some measurements are taken: First, both the FT-IR spectrum of pure PEG-6000 and that of $NiCl_2$–PEG complex are recorded (shown in Fig. 3a–b). It is found that most of the IR spectrum of PEG–$NiCl_2$ (Fig. 3b) is similar to that of pure of PEG (Fig. 3a) but there are two changes presented: (1) the vibration of C–O–C is slightly widened and shifts to higher wavenumbers; (2) the stretching vibration of associated hydroxyls shifts to lower wavenumbers. In Fig. 3a, the wavenumber v (~1104 cm^{-1}) is generated by the asymmetric stretching vibration of C–O–C, and due to the vibrational coupling effect of C–O–C, this peak splits. Now we concentrate on the phenomenon that the wavenumber v (~1104 cm^{-1}) corresponding to the vibration of C–O–C for pure PEG is shifted to ~1112 cm^{-1} for the PEG–$NiCl_2$ complex. Since the electron-negativity of oxygen atoms on PEG polymer is weakened *via* the partial donation of the oxygen lone pair electrons to the vacant d-orbit of Ni^{2+} ions, which makes the covalent properties of C–O–C increase, and thus leads the vibration constant and the bonding energy of C–O–C to increase, it is reasonable that the vibration of C–O–C shifts to higher wavenumbers. Furthermore, the absorption peak of C–O–C at ~1112 cm^{-1} has no obvious shift even though the PEG–$NiCl_2$ complex is washed with distilled water, demonstrating the coordinative chemical bonding of O: → Ni is relatively strong. Secondly, the transformation of the coordinative chemical effect between C–O–C and Ni^{2+} are investigated by FT-IR spectra as functions of temperature in the range of 30–200 °C, as shown in Fig. 3c–h. From Fig. 3c–h, the IR spectra transformation of the PEG–$NiCl_2$ complex is evident: because the PEG–$NiCl_2$ complex melts into the liquid phase above 60 °C, the vibration of C–O–C widens and the band around 3459 cm^{-1} disappears gradually with increasing the temperature, but the vibration of C–O–C is still positioned at ~1112 cm^{-1}, indicating that the coordinative chemical effect between PEG and $NiCl_2$ may exist under our experimental conditions.

Another change that arouses our interest is that v (~3459 cm^{-1}) in Fig. 3a corresponds to the stretching vibration of associated hydroxy while the corresponding vibration associated with hydroxy in Fig. 3b is shifted to a lower wavenumber, namely, v (~3435 cm^{-1}). It is well-known that if coordinative chemical bonding is formed between the –OH groups on the PEG terminal and Ni^{2+} ions, the vibration of the hydroxy ought to be moved to a lower wavenumber, and the stronger the strength of coordinative hydrogen bonding, the greater the decrease in wavenumber. So, it is possible that a coordinative effect between the –OH groups and $NiCl_2$ also occurs, which leads to a decrease in the vibration constant of O–H and thus makes the vibration of the associated hydroxy occur at a lower wavenumber.

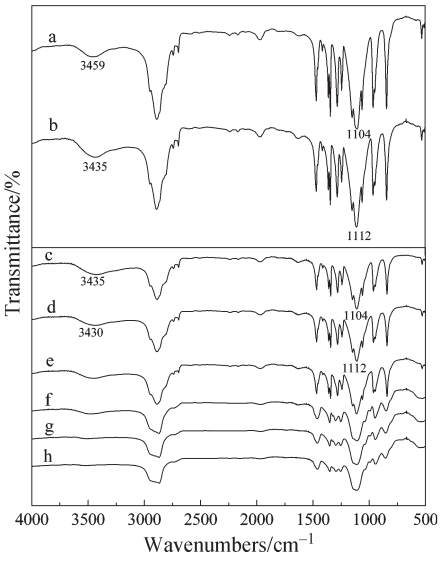

Fig. 3 (a) FT-IR spectrum of pure PEG-6000 polymer; (b) FT-IR spectrum of PEG–$NiCl_2$ complex and (c–h) FT-TR spectra as functions of temperature of the PEG–$NiCl_2$ complex: T = 30 °C, 50 °C, 60 °C, 70 °C, 150 °C, 200 °C, respectively.

Formation mechanism of complex architectures

The spatial conformations of the PEG–$NiCl_2$ complex most probably directly play an important role in the mineralization process. PEG-6000, as a non-ionic polymer, contains many hydrophilic (*i.e.* –C–O–C–, –OH) and hydrophobic (*i.e.* –CH_2–CH_2–) sites and the polymer chain has a very high flexibility due to the ease of rotation about C–O–C bonds. There are lone pair electrons on the oxygen atom of every repeating unit, and it should be noted that oxygen of the ether groups, according to Pearson, possesses strong basic properties, which provides the possibility that PEG polymer can combine with the Ni^{2+} ions to form PEG–$NiCl_2$ complex.[14] One PEG-6000 chain is composed of 135 ether oxygens and 2 –OH end groups (*i.e.* OH–[CH_2–CH_2–O]$_{135}$–CH_2–CH_2–OH), and realistically, it is very likely that an octahedral coordinated Ni^{2+} ion interacts with more than one PEG-6000 chain. According to Cai and Foulds' results,[15] one of the possible conformations of PEG–$NiCl_2$ complex can be schematized as in Fig. 4. It is exemplarily shown that Ni^{2+} ions can parasitize on the polymer backbones under the aid of functional groups on the PEG polymer. PEG backbone and Ni^{2+} ions would form a 3D framework under certain conditions, which provides the special macromolecular environment for the existence of Ni^{2+} ions. So, the renascent NiS nuclei, generated by the reaction of PEG–$NiCl_2$ complex with H_2S, may grow along this pre-obtained PEG–$NiCl_2$ complex framework. In addition, the tendency to form areas with high local metal complex concentration is proved to be intrinsic for a number of paramagnetic ions (Cu^{2+}, V^{4+}, Mo^{5+}, *etc.*).[16] When the first $NiCl_2$

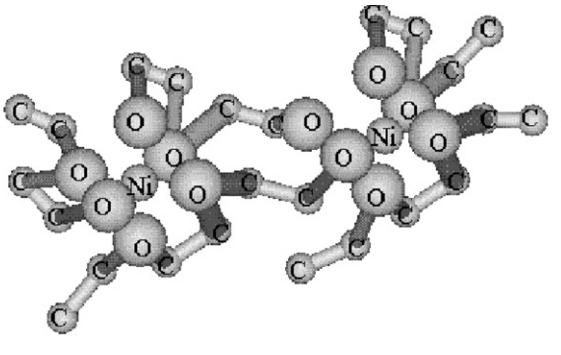

Fig. 4 Schematic representation of one of the possible conformations of PEG–$NiCl_2$ complex.

addition facilitates successive addition, interactions with the polymer chain will be completed only when all potentially active centers are occupied. The presence of polymer chains either heavily loaded or almost unloaded with metal ions can be observed, and the principle of "all or nothing" is realized.[16] The effect of "all or nothing" can generate the aggregation of renascent NiS nuclei, which makes the aggregated NiS nuclei grow along the pre-obtained 3D framework.

In the supplementary experiments, the procedure is similar except that PEG-6000 is substituted with other PEG polymers (the molecular weight in the range of 400∼2000 or $>10\,000$). The growth of the flower-like architecture is not favored in the mineralization process under these experimental conditions; the flower-like architectures cannot be built in the absence of PEG-6000 polymer. Furthermore, in our present systems, $CH_3COOC_4H_9$ is a good solvent for PEG, favoring the full extension of the polymer chain, while H_2O is a poor solvent for PEG, resulting in curling of the polymer chain. The coordinative effect of extension-curl would favor the formation of a 3D framework. Combining the above facts, it is evident that only when the network of PEG–$NiCl_2$ complexes is to the appropriate degree can it have a considerable influence on the formation of 3D architectures.

On the other hand, from the viewpoint of crystal structure, because the anisotropic nature of the building blocks in the hexagonal NiAs-type crystal structure, such as MS (M = Ni, Co), directs the formation of sheet-like structure, it is possible to form more complicated architectures, such as the tube.[10*b*] These sheet-like structures, grown from the aggregated particles, will grow larger and larger during the following hydrothermal process. Under the influence of 3D framework, these sheets may begin to curl (the interaction between the neighboring sheets could be reduced from the edges of the sheet, while keeping the interaction of the in-sheet atoms or molecules.) and the pre-obtained 3D framework may serve as the morphology-director for the growth of such complex architectures. Here, it is assumed that both the framework structure of PEG–$NiCl_2$ complex and the nature of the crystals play an important role in restricting crystallization of NiS in some directions but not others, where the aggregation of the sheet-like primary crystals leads to 3D flower-like micrometer-sized architectures. In other words, this 3D growth of crystals maybe is the outward embodiment of the internal crystal structure. FE-SEM observations (Fig. 5) of the immature products are obtained *via* a similar process except for a short reaction time (3 h and 6 h, respectively), revealing that the flower-like architectures are evolved from the primary particles and pass through a semi-flower transition. The appearance of the sheets can be observed from Fig. 5b. Combined with Fig. 1b–c, these results support the proposed morphology-directing mechanism. Although the concrete role of PEG-6000 in the solvothermal process is still not clear, the above-mentioned facts maybe allow us to assume that the framework structure of the PEG–$NiCl_2$ complex plays the role of the crystal morphology-directing and influences the fine geometrical details of the NiS nucleation and growth. This process could be called "crystal design/engineering".[17,18] The morphology-directing mechanism of the PEG–$NiCl_2$ complex seems to be of an intricate nature because NiS nucleation and the interaction of $NiCl_2$ with PEG-6000 can be expected to happen simultaneously.

In order to confirm the morphology-directing effect of the polymer–metal complex, we also attempt to substitute PEG-6000 with other polymers in our supplementary experiments, such as poly(vinyl alcohol) (PVA) and poly(vinyl pyrrolidone) (PVP). In the case of PVA, the coordinated atoms are hydroxy oxygens, and in the PVA–$NiCl_2$ complex it is assumed that each nickel ion tetrahedrally coordinates four hydroxy groups of PVA, two of them being protonated. Whereas as for PVP, the coordinated atoms are oxygen on carboxide and the heteroatoms adjoining (N atoms) on the pyrrolidone ring, although the exact coordinating bond geometry is still not very clear.[19] NiS crystals with tennis-ball morphology (shown in Fig. 6) and urchin-like architectures (shown in Fig. 7) are obtained, respectively, revealing the remarkable influence of the nature of the functional groups (–OH) on PVA polymer and that of functional groups (C=O, N) on PVP polymer.

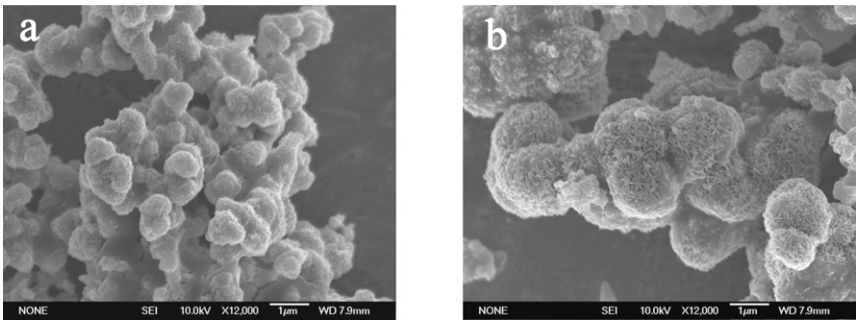

Fig. 5 FE-SEM images of the immature NiS powders obtained under a similar process (as involved in PEG) but with shorter reaction times: (a) 3 h (b) 6 h.

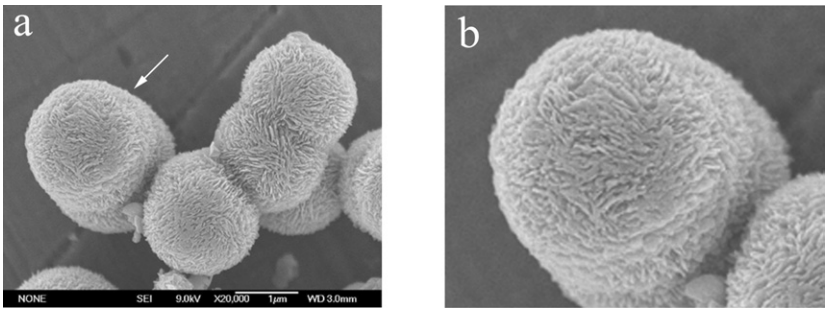

Fig. 6 (a) FE-SEM image of the NiS with tennis-ball architectures obtained using PVA polymer; (b) a high-magnification FE-SEM image of the section arrowed in (a).

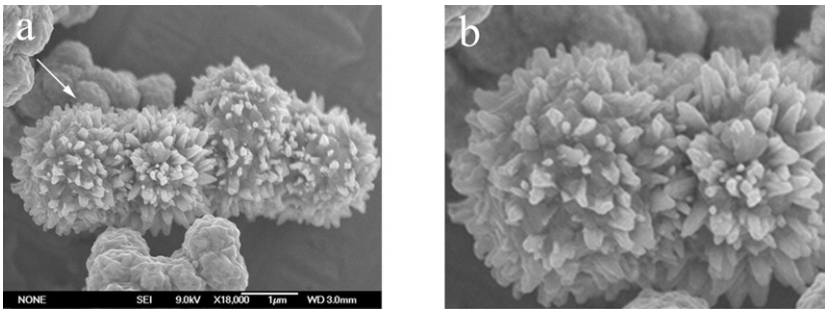

Fig. 7 (a) FE-SEM image of the urchin-like NiS architectures prepared in the presence of PVP polymer; (b) FE-SEM image under a higher magnification of the section arrowed in (a).

Due to the difference between octahedral and tetrahedral coordination environments, the framework structure of PEG–$NiCl_2$ complex and that of PVA–$NiCl_2$ complex generates the different morphology-directing effect. For instance, flower-like architectures are composed of larger sheets, while tennis-ball shaped architectures are composed of small sheets. It is evident that larger sheets have higher surface energy than small sheets and the higher surface energy is the driving force for the larger sheets to curl. Furthermore, in Fig. 6a, an interesting feature of the NiS architectures investigated is that some twin architectures with almost equal size can be observed, which is also a fact that can be explained by the special interaction of the functional groups on polymers with the growing nuclei as described above. A comparison of these three polymers indicates that the distance from donor atoms to polymer backbone has a considerable effect on their complex forming abilities, and it is obvious that the effectiveness of the functional groups differs with respect to the control of the crystal morphology. Polymer–$NiCl_2$ complex, depending on the kind of macromolecular environment, can also show labile, unsaturated and stained coordination structures. The multiple and dynamical interactions between a polymer matrix and a moiety strongly control the formation of highly ordered structures. Not only is the internal crystal structure of importance, but also the framework structure of polymer–$NiCl_2$ complex influences the formation of 3D architectures in the mineralization process. NiS crystals, directed by the framework structure of the polymer–$NiCl_2$ complex, grow in the direction where the crystallization hindrance is weakest.

Conclusions

In summary, a complex-ion reaction under solvothermal conditions at ~150 °C for ~12 h was carried out for the preparation of 3D NiAs-type α-NiS with complex architectures, on the basis of the strategy that the framework structure of polymer–$NiCl_2$ complex could provide the orientation for the growth of 3D NiS crystals. It was found that both the framework structure of polymer–$NiCl_2$ complex and the functional groups on the polymers (*i.e.*–C–O–C–, –OH, C=O, N) played a crucial role in the final architectures of NiS. Since the polymers can extend the possibilities of inorganic morphogenesis, this approach is expected to form a general route to exert control over mineralization growth of the transition metal sulfides in restricted dimensions with controllable size. By varying the functional groups on the polymers and by using a suitable solvent, more specific morphology-directors become available for the appearance of other complex architectures.

Acknowledgements

Financial supports from the National Natural Science Foundation of China, Chinese Ministry of Education and Chinese Academy of Sciences are gratefully acknowledged.

References

1 (*a*) B. A. Korgel and D. Fitzmaurice, *Adv. Mater.*, 1998, **10**, 661; (*b*) L. L. Beecroft and C. K. Ober, *Chem. Mater.*, 1997, **9**, 1302; (*c*) C. B. Murray, C. R. Kagan and M. G. Bawendi, *Science*, 1995, **270**, 1335.
2 (*a*) C. A. Mirkin, R. L. Letsinger, R. C. Mucic and J. J. Storhoff, *Nature*, 1996, **382**, 607; (*b*) O. Vidoni, K. Philippot, C. Amiens, B. Chaudret, O. Balmes, J. O. Malm, J. O. Bovin, F. Senocq and M. Casanove, *Angew. Chem. Int. Ed.*, 1999, **38**, 3736; (*c*) S. Mann and G. A. Ozin, *Nature*, 1996, **382**, 313.
3 (*a*) W. Z. Wang, G. H. Wang, X. S. Wang, Y. J. Zhan, Y. K. Liu and C. L. Zheng, *Adv. Mater.*, 2002, **14**, 67; (*b*) W. Z. Wang, Y. J. Zhan and G. H. Wang, *Chem. Comm.*, 2001, 727.
4 (*a*) J. J. Zhu, X. H. Liao, X. N. Zhao and H. Y Chen, *Mater. Lett.*, 2001, **49**, 91; (*b*) S. J. Chen, X. T. Chen, Z. L Xue, L. H. Li and X. Z. You, *J. Cryst. Growth*, 2002, **246**, 169; (*c*) C. Santato, M. Odziemkowski, M. Ulmann and J. Augustynski, *J. Am. Chem. Soc.*, 2001, **123**, 10 639.
5 (*a*) Y. J. Xiong, Y. Xie, C. Z. Wu, J. Yang, Z. Q. Li and F. Xu, *Adv. Mater.*, 2003, **15**, 405; (*b*) F. Xu, X. Zhang, Y. Xie, X. B. Tian and Y. Z. Li, *J. Colloid Interface Sci.*, 2003, **260**, 160.
6 (*a*) L. M. Qi, H. Cölfen and M. Antonietti, *Angew. Chem. Int. Ed.*, 2000, **39**, 604; (*b*) S. H. Yu, M. Antonietti, H. Cölfen and M. Giersig, *Angew. Chem. Int. Ed.*, 2002, **41**, 2356.
7 (*a*) S. H. Yu, H. Cölfen and M. Antonietti, *Adv. Mater.*, 2003, **15**, 133; (*b*) D. B. Zhang, L. M. Qi, J. M. Ma and H. M. Cheng, *Chem. Mater.*, 2002, **14**, 2450.
8 (*a*) W. S. Sheldrick and M. Wachhold, *Angew. Chem. Int. Ed.*, 1997, **36**, 207; (*b*) B. O. Dabbousi, M. G. Bawendi, O. Onitsuka and M. F. Rubner, *Appl. Phys. Lett.*, 1995, **66**, 1316.
9 (*a*) J. T. Sparks and T. Komoto, *Rev. Mod. Phys.*, 1968, **407**, 52; (*b*) D. B. WcWhan, M. Marezio, J. P. Remeika and P. D. Darnier, *Phys. Rev. B*, 1972, **5**, 2552; (*c*) E. Wong, C. W. Sheeleigh, and S. B. Rananvare, *Proceedings of the Sixth Annual Conference on Fossil Energy Materials*, NETL Publications, 1992, p. 143.
10 (*a*) C. B. Lioutas, C. Manolikas, G. Van Tendeloo and J. Van Landuyt, *J. Cryst. Growth*, 1993, **126**, 457; (*b*) X. C. Jiang, Y. Xie, J. Lu, L. Y. Zhu, W. He and Y. T. Qian, *Adv. Mater.*, 2001, **13**, 1278; (*c*) A. M. Fernandez, M. T. S. Nair and P. K. Nair, *Mater. Manuf. Processes*, 1993, **8**, 535.
11 (*a*) B. Xie, Y. Jiang, S. W. Yuan, Q. Li, Y. Wu, J. Wu and Y. T. Qian, *Chem. Lett.*, 2002, 254; (*b*) X. M. Zhang, C. Wang, Y. Xie and Y. T. Qian, *Mater. Res. Bull.*, 1999, **34**, 1967.
12 C. D. Wagner, W. W. Riggs, L. E. Davis, J. F. Moulder and G. E. Muilenberg, *Handbook of X-ray Photoelectron Spectroscopy*, Perkin–Elmer Corporation, Physical Electronics Division, USA, 1979.
13 M. Nakamura, A. Fujimori, M. Sacchi, J. C. Fuggle, A. Misu, T. Mamori, H. Tamura, M. Matoba and S. Anzai, *Phys. Rev. B*, 1993, **48**, 16 942.
14 P. G. Pearson, *J. Chem. Educ.*, 1963, **45**, 581.
15 (*a*) H. Cai and G. C. Farrington, *J. Electrochem. Soc.*, 1992, **139**, 744; (*b*) G. A. Foulds, *Coord. Chem. Rev.*, 1995, **146**, 153.
16 F. Ciardelli, E. Tsuchida, D. Wöhrle, *Macromolecule-Metal Complexes*, Springer, Berlin, 1996.
17 (*a*) L. Addadi, Z. Berkovitch-Yellin, I. Weissbuch, M. Lahav and L. Leiserowitz, *Top. Stereochem.*, 1986, **16**, 1; (*b*) S. N. Black, L. A. Bromley, D. Cottier, R. J. Davey, B. Dobbs and J. E. Rout, *J. Chem. Soc., Faraday Trans.*, 1991, **87**, 3409.
18 (*a*) H. E. Buckley, *Z. Kristallogr.*, 1935, **91**, 375; (*b*) B. Raistrick, *Discuss. Faraday Soc.*, 1949, **40**, 234; (*c*) J. Whetstone, *Discuss. Faraday Soc.*, 1954, **16**, 132.
19 (*a*) Y. G. Sun and Y. N. Xia, *Science*, 2002, **298**, 2176; (*b*) F. Bonet, K. Tekaia-Elhsissen and K. V. Sarathy, *Bull. Mater. Sci.*, 2000, **23**, 165.